J Solid State Electrochem (2009) 13:849–859
DOI 10.1007/s10008-008-0598-z

ORIGINAL PAPER

Comparison between different ways to determine diffusion coefficient and by solving Fick's equation for spherical coordinates

A. Dell'Era · M. Pasquali

Received: 20 February 2008 / Accepted: 20 May 2008 / Published online: 14 July 2008

Abstract The following document covers the determination of the diffusion coefficient of two powder materials: $LiFePO_4$ and $LiMn_2O_4$ by using potentiostatic intermittent titration technique (PITT) and impedance spectroscopy methodology and compares relevant results with the following relation: $D = \frac{R^2 I_0}{3\alpha Q}$, which is obtained by solving Fick's spherical coordinate equation (where I_0 is the initial step current in the PITT experiment, R is the particle radius, Q is the charge that intercalated during the step, and α is the percentage of the theoretical intercalated charge). This procedure allowed the verification of the validity of the spherical model for the powder materials, the accuracy of the expression proposed for the diffusion coefficient determination, and the correctness of the measures that had been taken.

Keywords Lithium iron phosphate · Lithium manganese oxide spinel · Diffusivity · Spherical geometry model

Introduction

Based on the procedure preparation, some literature considers electrodes as a single part of the electrochemical system referring to the diffusivity phenomena, and the thickness of the electrode is considered as the characteristic length to use in the calculation of the diffusion coefficient [1]. This work intends, instead, to highlight the different corpuscular nature of the electrode consisting of various materials mixed together and therefore the different approach aiming at taking into account the diffusivity phenomena. In literature, there exists various models similar to the one proposed in this paper, but they do not reach the same expression to calculate the diffusion coefficient. In fact, they are also functions of different parameters. Other authors [2–5], even if they use a spherical geometry to approach the diffusion phenomena, do not propose an expression in which the parameters can be simply measured. We proposed an expression of D, by resolving the Fick equation, during the potential step, with no approximation but calculating the equation resolution simply for $t=0$. We formalized the α role as ratio between the real charge intercalated and the theoretical capacity, close to the concept of ratio between galvanic and potentiostatic capacity [3] but without being the same concept. As regards to $LiFePO_4$, it is, also, important to specify that lithium intercalation/deintercalation is accompanied by strong electron–ion interactions, leading to the coexistence of two phases. This being the case, the insertion of lithium takes place by means of several reaction fronts, and a pseudo-diffusivity coefficient should more correctly be defined, despite McKinnon and Hearing's assumption [6] who found that it is not possible to distinguish between two different diffusion models based on continuous (solid solution formation) or noncontinuous (two-phase formation) charging procedures. For the construction of the electrode, a cathodic powder material was mixed with a conductive material and a binder to arrive to an electrode, macroscopically seen as a unit, but with a microscopic nature in its chemical and physical properties.

A. Dell'Era (✉) · M. Pasquali
Department of Chemical Engineering,
University of Rome "La Sapienza",
Rome, Italy
e-mail: alessandro.dellera@uniroma1.it

Fick's spherical coordinate equation resolution

To study the diffusion phenomena following the electrochemical process and occurring inside the particles of the active material used in the production of the electrode, the second Fick's law written in spherical coordinates has been considered.

$$\frac{\partial c}{\partial t} = D\frac{1}{r^2}\frac{\partial}{\partial r}\left(r^2\frac{\partial c}{\partial r}\right) \tag{1}$$

where D is the diffusion coefficient, c is the mobile specie concentration, r is the spherical coordinate, and t is the time.

The solution shall be the following as it is possible to verify in the Appendix:

$$c_s - c = \frac{(c_s - c_0)R}{\pi}\exp\left(-\frac{\pi^2}{R^2}Dt\right)\frac{\sin\left(\frac{\pi}{R}r\right)}{r} \tag{2}$$

Plotting Eq. 2 in Fig. 1, where R is the particle radius, the behavior of the difference in concentration between particle surface c_s and particle bulk c in function of the r/R ratio, taking the time t as parameter, is shown.

Knowing the concentration profile form, it is possible to work out for the current within one particle I_p, the following expression 3 according to the first Fick's law:

$$I_p(r,t) = \frac{(c_s - c_0)R}{\pi}\exp\left(-\frac{\pi^2}{R^2}Dt\right)\left[\frac{\cos\left(\frac{\pi\cdot r}{R}\right)\frac{\pi}{R}}{r} - \frac{\sin\left(\frac{\pi\cdot r}{R}\right)}{r^2}\right]$$
$$4\pi\cdot r^2\overline{n}FD \tag{3}$$

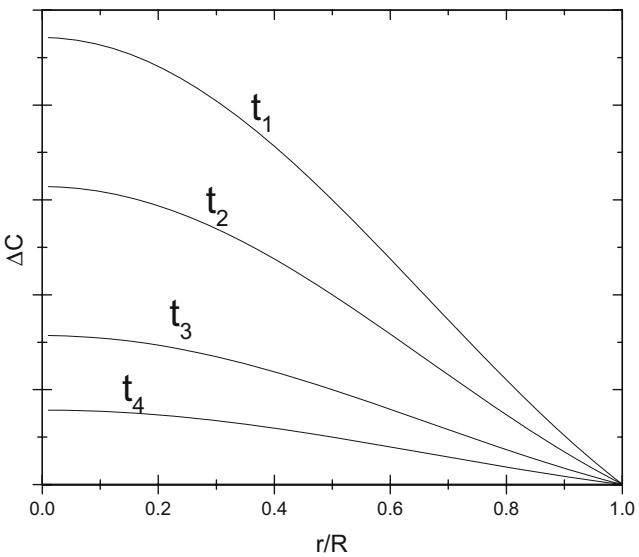

Fig. 1 Time-dependent profile concentration

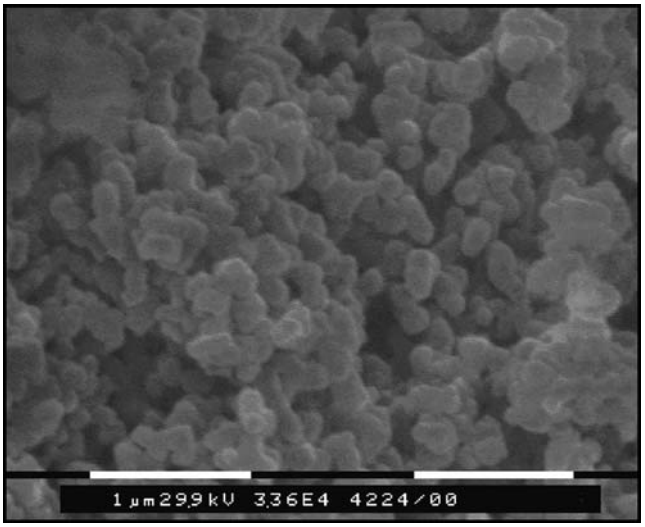

Fig. 2 $LiFePO_4$ SEM picture

where $\overline{n}$ is the ion lithium charge number and F is the Faraday's constant. With $r=0$, $I_p(0,t)=0$.

While when $r=R$ and $t\to 0$,

$$\left|I_{0p}\right| = (c_s - c_0)4\pi zFDR \tag{4}$$

And because of [7],

$$(c_s - c_0) = \frac{Q}{zFnV_M} = \frac{Q}{zFV_{tot}} = \frac{Q}{zFn_p\frac{4}{3}\pi R^3} \tag{5}$$

where n is the number of moles in the static component, V_M is the molar volume, n_p is the number of the particles, and Q is the total charge transferred during the titration corresponding to the voltage step.

For one particle, it shall be possible to write:

$$I_{0p} = \frac{3DQ}{n_pR^2} \tag{6}$$

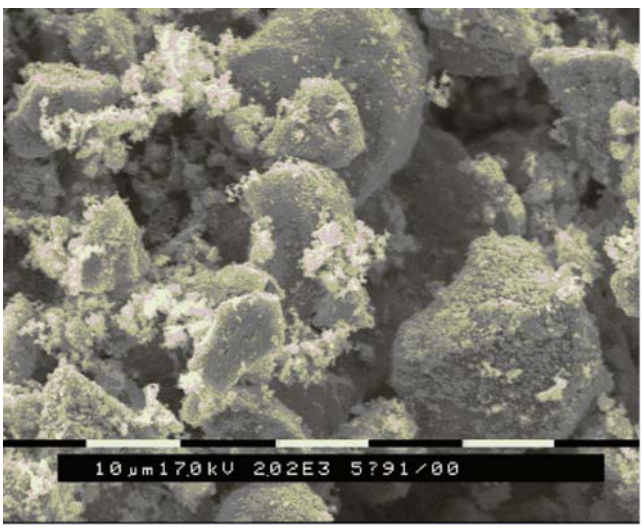

Fig. 3 $LiMn_2O_4$ SEM picture

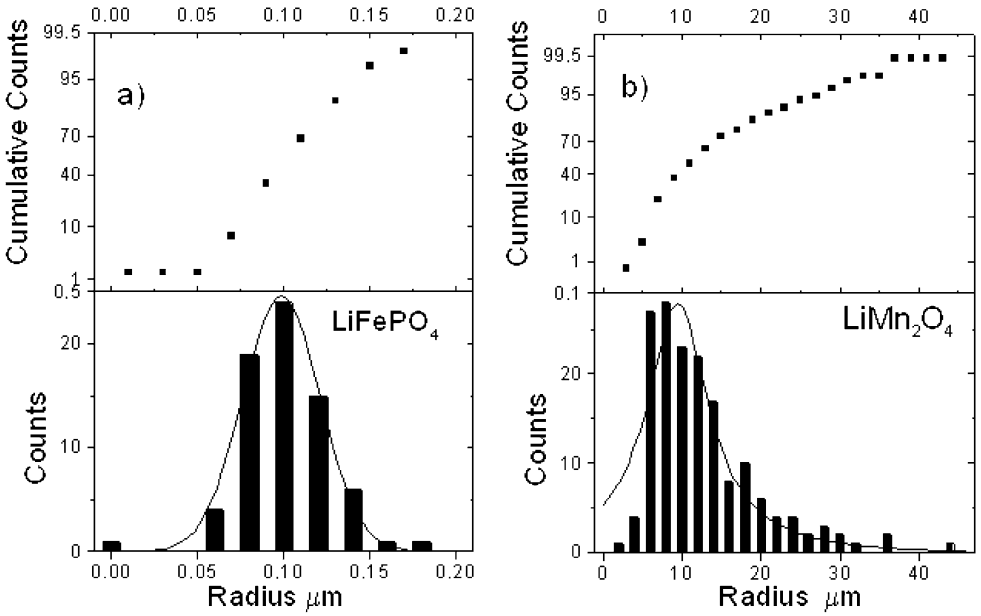

Fig. 4 Particle size distributions

defining α as the parts of the particles electrochemically active during the step voltage. The latter value is not equal for each step, but it is possible to assume reasonably α as the efficiency value of the overall charge transfer process, defined as the ratio between the real and theoretical value of the capacity. The total initial current of the step is:

$$I_0 = \frac{3DQ}{n_p R^2} \alpha n_p \tag{7}$$

and so:

$$D = \frac{R^2 I_0}{3Q\alpha} \tag{8}$$

Preparation samples

$LiFePO_4$ Preparation

Fe(II) methyl phosphonate $Fe((CH_3PO_3)(H_2O))$ (FeMP) and Fe(II) phenyl phosphonate $Fe((C_6H_5PO_3)(H_2O))$ (FePP), which is the precursors of $LiFePO_4$, have been synthesized as reported in [8]. The latter compounds can be isolated as white microcrystalline powders and are stable in air and moisture. Li_2CO_3 and FeMP or FePP were ball-milled at a ratio of 1:2 in air to get an intimate mixture. Gray powders of $LiFePO_4$ were obtained by heating the precursor mixtures in a tubular furnace under inert atmosphere (N_2 gas) at temperatures above 600 °C for at least 16 h.

$LiMn_2O_4$ preparation

Powder samples of $LiMn_2O_4$ composition have been prepared by heating at 730°C a mixture of stoicheiometric amounts of the relevant metal oxides and Li_2CO_3. The components of the mixture were ball-milled for 1 h and then transferred to an oven, where they were left 72 h in the air at 730 °C. Slow cooling was always applied [9, 10].

Characterization samples

A characterization of synthesized powders has been effected by some techniques such as scanning electron microscopy (SEM), Brunauer-Eramett-Teller (BET), and X-ray diffraction (XRD) analysis. By the first one, a valuation of the particles size has been possible for $LiFePO_4$ and $LiMn_2O_4$ as it results in Figs. 2 and 3, respectively. Moreover, a statistical analysis of SEM images has been made by using a useful software specialized in images elaboration: DIGIMIZER. In Fig. 4a,b, the distributions of

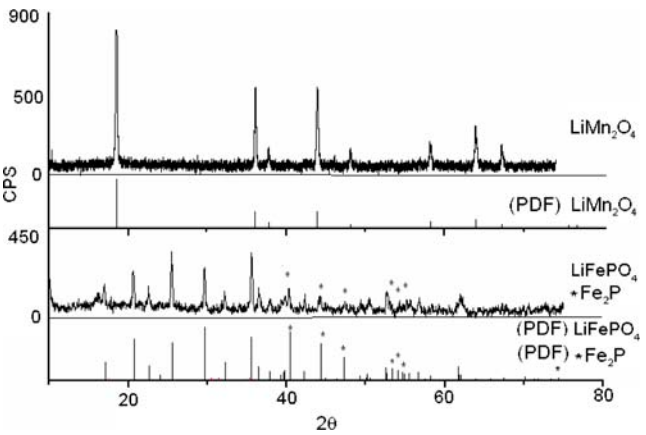

Fig. 5 $LiFePO_4$ and $LiMn_2O_4$ XRD patterns

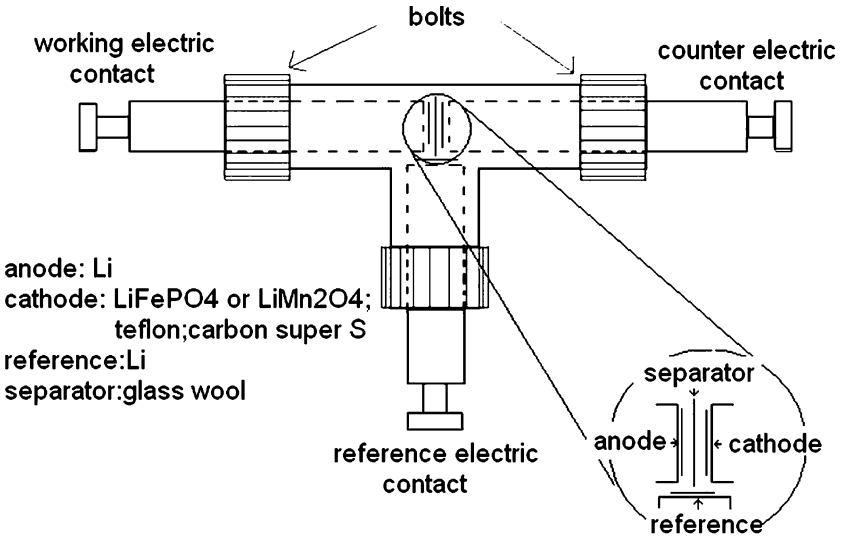

Fig. 6 Electrochemical cell

particles size are shown, by which it is possible to determine the mean value of radius for both materials. Our BET measurements on synthesized spinels showed mean values of 3.0 m^2/g, in accord with literature data [11, 12], while for $LiFePO_4$, the mean value is 110 m^2/g, but it is necessary to consider that, in this case, the measure is affected by the presence of amorphous carbon forming during the synthesis. In Fig. 5 the XRD patterns for both materials have been reported. Comparing the patterns with the data taken from the powder diffraction file, we verified the goodness of the synthesis, even if, for the lithium iron phosphate, a small quantity of the Fe_2P phase has been recognized. Finally, by the shape of the peaks, a certain level of crystallinity for both materials has been deduced.

Experimental system

After sample preparation, cathode electrodes have been prepared for a subsequent use in the electrochemical system described below. Therefore, the powder with a conductive material, such as carbon Super, and with a binder, like Teflon, was mixed and pounded together by a pestle in a mortar and then laminated. Using a socket punch, an electrode having a

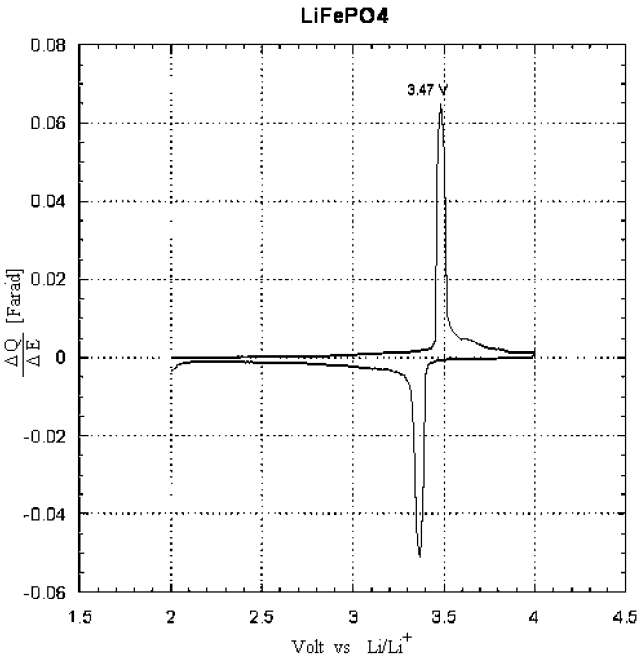

Fig. 7 $LiFePO_4$ potential step cyclic voltammetry

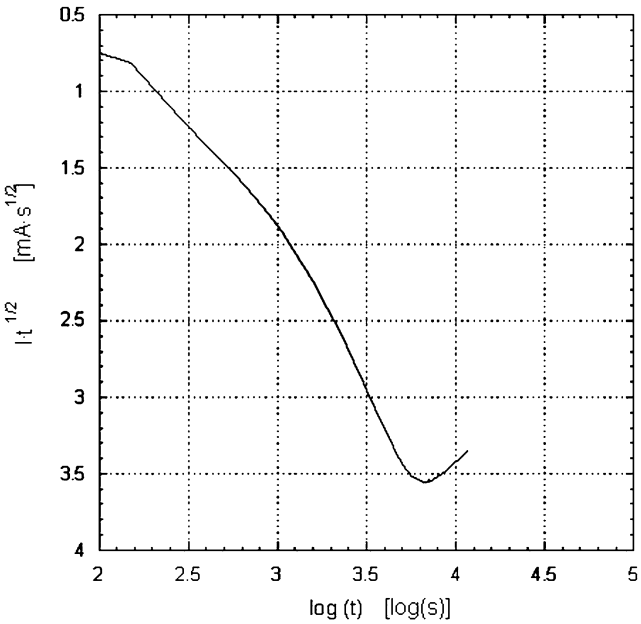

Fig. 8 Cottrell region for $LiFePO_4$

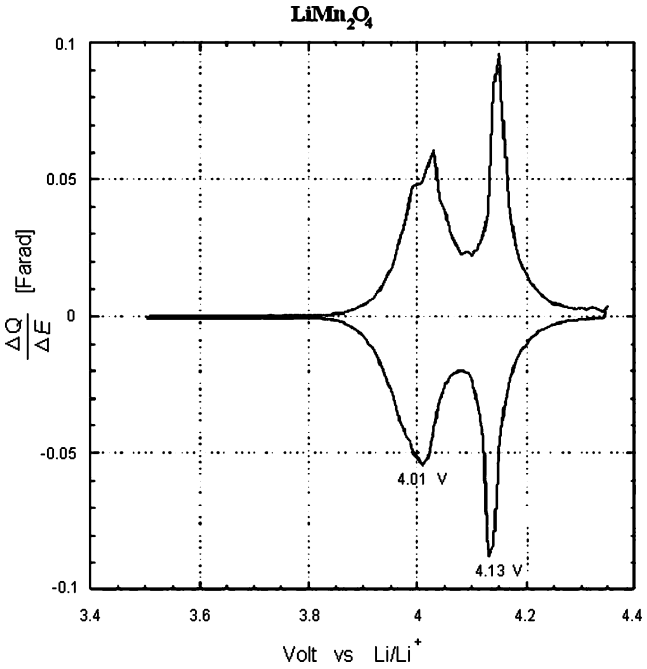

Fig. 9 $LiMn_2O_4$ potential step cyclic voltammetry

surface of about 0.7 cm^2 has been made and put as a cathode in the cell reported at Fig. 6, where the anode is metallic lithium, the separator is glass wool, and the electrolyte is a solution of dimethyl carbonate and ethylene carbonate (1:1 molar) as solvents and $LiPF_6$ as the solute.

Finally, this electrochemical system has been used in experiments with the frequency response analyzer and with the potentiostat–galvanostat to determine the diffusion coefficient. In our experiment, the diffusion coefficient of such different materials has been calculated, at room temperature, on the first-sweep oxidation peak for $LiFePO_4$ and on the first-sweep reduction peaks for $LiMn_2O_4$, by using a Mac-Pile-II Biologic potentiostat–galvanostat. In all experiments, the relaxation open circuit was 20 s and the step duration 10 s if I_0<0.01 mA.

For the impedance spectroscopy, the hardware we used consisted of a frequency response analyzer (Solartron 1255 HF model) and an electrochemical interface module (Solartron 1286 model) by EG & G, while a Zplot program has been used as the software.

Determination of the diffusion coefficient

PITT technique [13]

The first-sweep oxidation peak for $LiFePO_4$ is about 3.47 V, as it is possible to see in Fig. 7. In this picture, the intercalation–deintercalation process can be observed in correspondence of two peaks. The upward one is the oxidation process at approximately 3.47 V (odd sweeps), while the downward peak is the reduction process at approximately 3.38 V (even sweeps). Plotting $I\sqrt{t}$ vs. log (t), where I is the current value during the potential step at 3.47 V, it is possible to specify a particular region where $I\sqrt{t}$ is almost constant and highlights a Cottrell behavior. Under this condition, the follow expression [7, 14] is valid within the Cottrell region:

$$I(t)\sqrt{t} = \frac{QD^{1/2}}{L\pi^{1/2}} \tag{9}$$

where Q is the charge intercalated during the step, L is the characteristic diffusion length, D is the diffusion coefficient, and I is the current during the step. It has been assumed that—as regards this material—the characteristic diffusion length, L, is approximately equal to the radius value, i.e., of about 0.1×10^{-4} cm, as reported by Fig. 2. Therefore, by the Cottrell region individuation in Fig. 8:

$$I\cdot\sqrt{t} = \frac{\sqrt{D}Q}{\sqrt{\pi}R} \tag{10}$$

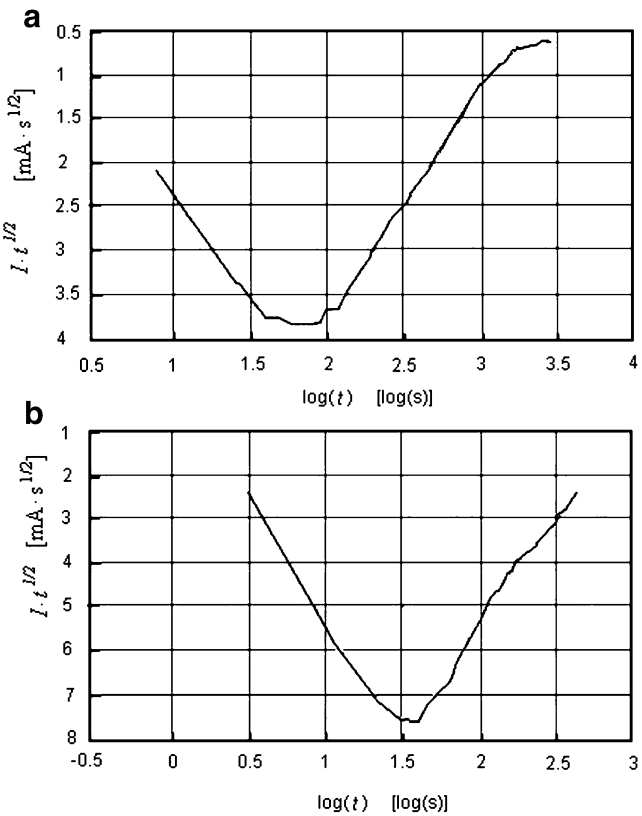

Fig. 10 **a** Cottrell region for $LiMn_2O_4$ at 4.01 V; **b** Cottrell region for $LiMn_2O_4$ at 4.13 V

Table 1 Cottrellian parameters to adjust the diffusion coefficient measured by Cottrell region individuation

Method	Parameter	$LiFePO_4$ 3.47 V	$LiMn_2O_4$ 4.01 V	$LiMn_2O_4$ 4.13 V
PITT and Cottrell region	$\log(\Lambda)$	2	0.36	0.3
PITT and Cottrell region	D_{ap}/D	1	0.6	0.55
PITT and Cottrell region	D (cm^2/s)	3.2×10^{-14}	2.6×10^{-9}	5.2×10^{-9}

is possible to calculate the diffusion coefficient for the $LiFePO_4$ material [15]. The same procedure has been followed for $LiMn_2O_4$. Therefore, we started from the potential-step cyclic voltammetry to identify two reduction peaks of the odd weeps (first sweep). The first peak is at 4.01 V and the second one at 4.13 V, as reported by Fig. 9 (downward peaks). For $LiMn_2O_4$, the first sweep is a discharge process. As seen before, $LiMn_2O_4$ particles are much bigger than $LiFePO_4$ particles, and it has been assumed that the characteristic diffusion length in this case is equal to approximately 10×10^{-4} cm, as it is possible to see in Fig. 3.

Plotting $I\sqrt{t}$ vs. $\log(t)$, as before, two Cottrell regions (Fig. 10a,b) have been determined, i.e., one region per each oxidation peak of the said material. In this case, two diffusion coefficients have been evaluated at 4.01 and 4.15 V.

As Montella highlighted in his work [16], it is possible, in many cases, that the diffusion coefficient, calculated determining the Cottrellian region, can be underestimated, and to calculate the real diffusion coefficient, it is necessary to evaluate the dimensionless parameter Λ defined as [17, 18]:

$$\Lambda = \frac{R_d}{R_\Omega + R_{ct}} \tag{11}$$

where R_d is diffusion resistance, R_Ω is the ohmic resistance, and R_{ct} is the charge transfer resistance. The expression connecting the diffusion coefficient D to the parameter Λ is [16]:

$$\frac{D_{ap}}{D} = 4\frac{b^2}{\pi^2} \tag{12}$$

where D_{ap} is apparent diffusion coefficient and b is [16]: $b = \frac{\pi}{2}$ for high values of Λ; $\log(\Lambda)>1$. When Λ has high values, the intercalation process is under diffusional control and $D_{ap}=D$. For values of $\log(\Lambda)$ between the range $[-1.2; 1]$, the following expression is valid [16]:

$$b\tan(b) - \Lambda = 0 \tag{13}$$

Instead, for very low values of Λ

$$b = \sqrt{\Lambda} \tag{14}$$

[16]

Vorotyntsev et al. [18] recognized an expression linking the parameter Λ to other potential step parameters:

$$\Lambda = \frac{I(0)\cdot\tau_d}{\Delta Q} \tag{15}$$

where $I(0)$ is the initial current of the step, ΔQ is the intercalated charge during the step and τ_d is the diffusion time constant defined as [14, 16–18]:

$$\tau_d = \frac{L^2}{D} \tag{16}$$

Montella, in his work, first evaluated the diffusion resistance by the electrochemical impedance spectroscopy (EIS) technique, to use it in the individualization of the parameter Λ. With the same focus, we first determined the diffusion coefficient by EIS technique, to then calculate, assuming the mean particle radius as characteristic length L, the diffusion time constant τ_d through the expression 16 and, by the potential step parameters and the expression 15, the parameter Λ, for both materials. By various experi-

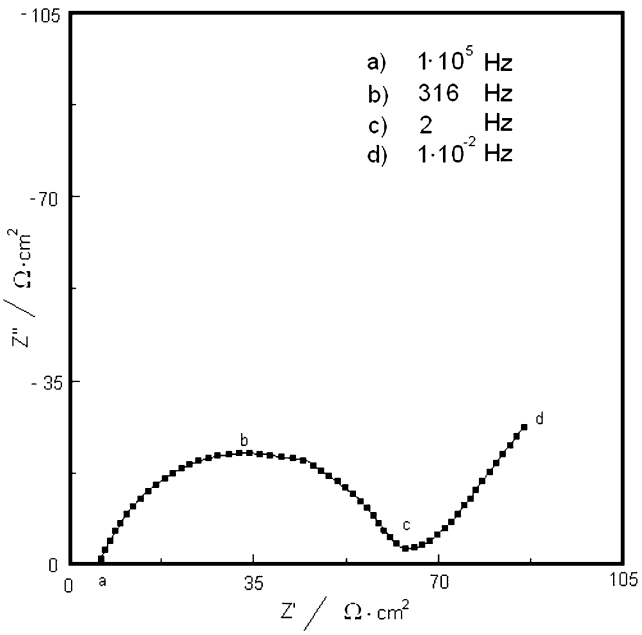

Fig. 11 $LiFePO_4$ impedance spectroscopy: real and imaginary components of the complex impedance at 3.47 V

Table 2 Parameters measured by impedance spectroscopy for $LiFePO_4$

Method	$LiFePO_4$ 3.47 V D (cm^2/s)	$LiMn_2O_4$ 4.01 V D (cm^2/s)	$LiMn_2O_4$ 4.13 V D (cm^2/s)
Impedance spectroscopy	2.0×10^{-14}	3.7×10^{-9}	2.3×10^{-9}

ments, the parameters $I(0)$ and ΔQ have been measured and the mean value of the parameter Λ has been determined. Finally, in Table 1, the $\log(\Lambda)$, the $\frac{D_{ap}}{D}$, and the corrected diffusion coefficient values have been reported for $LiMn_2O_4$ and $LiFePO_4$.

Impedance spectroscopy technique

For our two different materials, through the application of a different technique, almost the same value of the diffusion coefficient has been found, at the same potential value as before. In Fig. 11 (Nyquist diagram), the real and quadrature components of impedance have been reported for lithium iron phosphate at 3.47 V, in correspondence of the previously seen charge peak. In Tables 2 and 3, the parameters found by the impedance spectroscopy technique, for such material, have been reported.

The electrolytic resistance R_{el} is the first intercept of the semicircle with the X-axis, while the second intercept is the sum of the electrolytic resistance R_{el} and the polarization resistance $\sum_i R_{pi}$ where i is the number of semicircles and R_s is the intercept of the Warburg straight line sloping at approximately 45° with the X-axis. Finally, C is the double-layer capacitance. The real component of impedance is [19]:

$$Z_{real} = R_{el} + R_{ct} - 2C\sigma^2 \tag{17}$$

Where σ is [19]:

$$\sigma = \frac{V_M \partial E/\partial y}{nFS\sqrt{2D}} \tag{18}$$

In the above expression, V_M is the molar volume, n are the electron moles for each mole of intercalated specie, $\partial E/\partial y$ is the potential derivate with respect to the intercalation degree, and D is the diffusion coefficient. The value of S should be considered as the real surface, but, like other authors, we assume S as the electrode geometric surface [20, 21]. As a matter of fact, calculations of the diffusion coefficients were based on the geometrical area, accepting that this may be underestimated due to the rough surface. Figure 12a shows the discharge curve of $LiFePO_4$ as a function of the intercalation degree (E vs. y) and its derivate ($\frac{dE}{dy}$). The intercalation value at 3.47 V, on the peak reported by Fig. 7, is 0.65, and increasing the picture

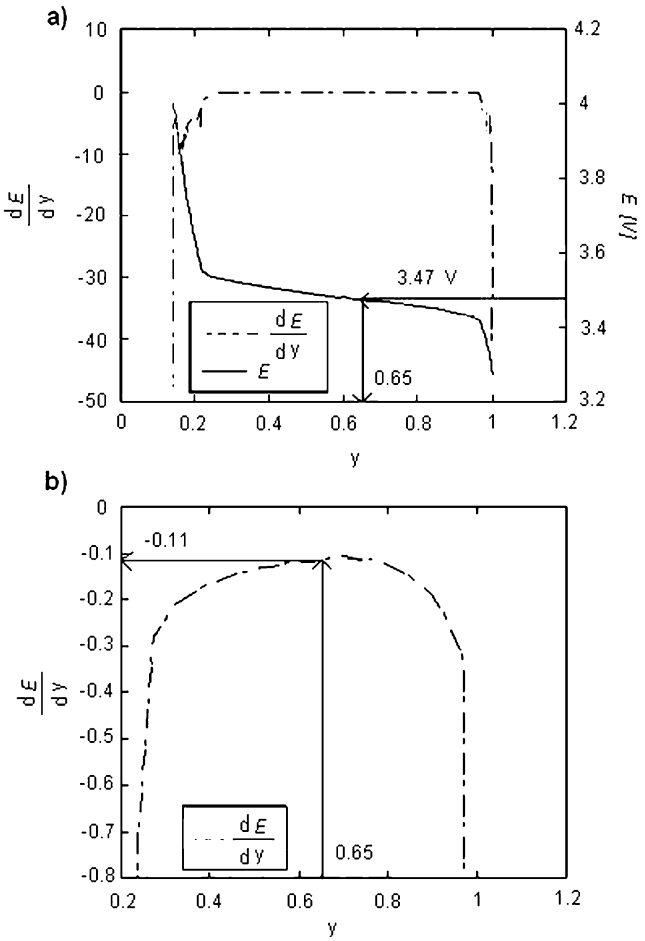

Fig. 12 **a** Discharge curve of the $LiFePO_4$ as function of the intercalation degree (E vs. y) and its derivate ($\frac{dE}{dy}$); **b** high-resolution of discharge curve derivate

Table 3 Parameters measured by impedance spectroscopy for $LiFePO_4$

	r_{el} ($\Omega\cdot cm^2$)	$r_{el}+r_{p1}$ ($\Omega\cdot cm^2$)	r_s ($\Omega\cdot cm^2$)	C (F/cm^2)
3.47 V	4.3	64.5	63.8	6.8×10^{-6}

Table 4 Calculated coefficient diffusion values for $LiMn_2O_4$ by impedance spectroscopy

	r_{el} ($\Omega\cdot cm^2$)	$r_{el}+r_{p1}+r_{p2}$ ($\Omega\cdot cm^2$)	r_s ($\Omega\cdot cm^2$)	C (F/cm^2)
4.01 V	3.8	12.6	12.5	6.1×10^{-2}
4.13 V	3.8	11.4	11.1	5.7×10^{-2}

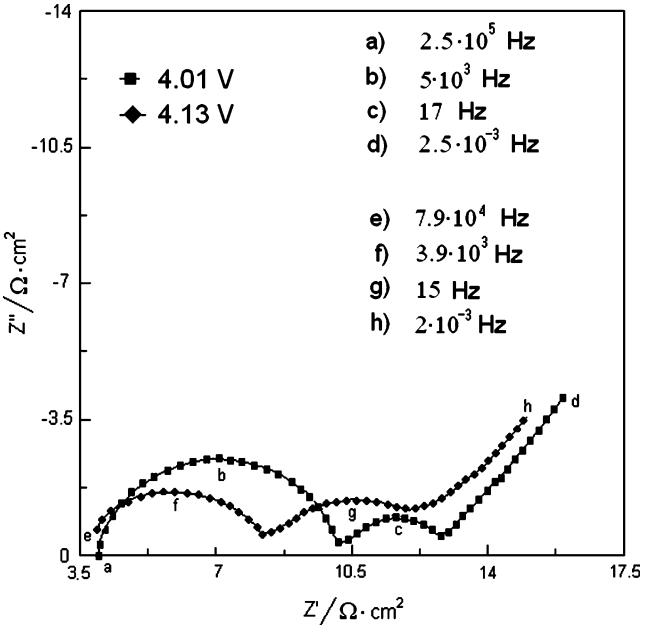

Fig. 13 $LiMn_2O_4$ impedance spectroscopy: real and imaginary components of the complex impedance; at 4.01 and 4.13 V

Table 5 Voltage step parameters for $LiFePO_4$ and $LiMn_2O_4$

	V	I_0 (mA)	ΔQ (mAh)	α
$LiFePO_4$	3.47	0.111	0.098	0.88
$LiMn_2O_4$	4.01	1.3	0.047	0.8
$LiMn_2O_4$	4.13	1.85	0.068	0.8

resolution, it is possible to determine the value of the derivate graphically as it is possible to see in Fig. 12b.

These parameters can be used inside expression 17. In this case, the module of the derivate value is equal to 0.11, and considering that the surface of the electrode is of approximately 0.7 cm^2, the $LiFePO_2$ molar volume is of 40.2 cm^3/mol, and the Faraday's constant is equal to 96,485 C, it is possible to use it in expression 18.

In this way, the diffusion coefficient value has been calculated and reported in Table 2.

Following the same procedure for $LiMn_2O_4$, it has also been possible to calculate the diffusion coefficient for this material. In Fig. 13 (Nyquist diagram), the real and quadrature components of impedance have been reported

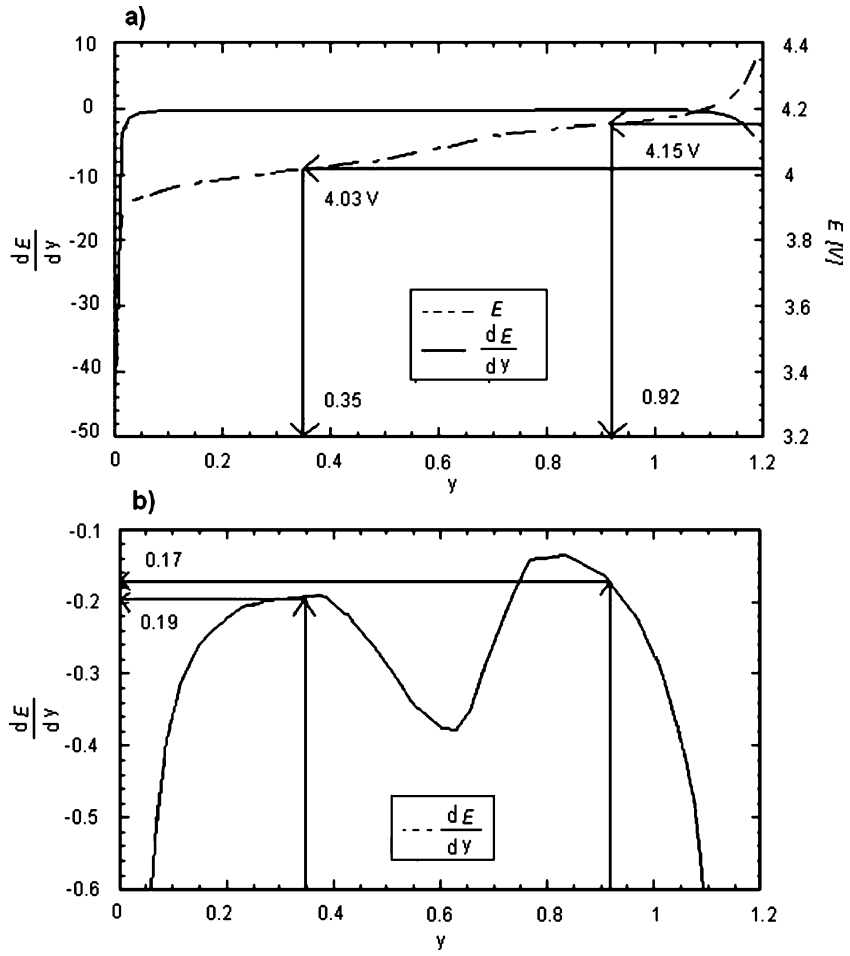

Fig. 14 **a** Discharge curve of the $LiMn_2O_4$ as function of the intercalation degree (E vs. y) and its derivate ($\frac{dE}{dy}$); **b** high-resolution of discharge curve derivate

Table 6 Calculated coefficient diffusion values for $LiMn_2O_4$ and $LiFePO_4$ by spherical coordinate Fick equation resolution

Method	$LiFePO_4$ 3.47 V D (cm^2/s)	$LiMn_2O_4$ 4.01 V D (cm^2/s)	$LiMn_2O_4$ 4.13 V D (cm^2/s)
PITT and SCFER	1.2×10^{-14}	3.2×10^{-9}	3.1×10^{-9}

for spinel at 4.01 and 4.13 V, while in Table 4, the parameters found by the impedance spectroscopy technique, for such material, have been also reported.

In Fig. 14a, it is possible to see the discharge curve of the $LiMn_2O_4$ as a function of the intercalation degree (E vs. y) and its derivate ($\frac{dE}{dy}$); the intercalation values at 4.01 and 4.13 V, in correspondence of the two reduction peaks shown in Fig. 9, are equal to 0.35 and 0.92 respectively, and by increasing the resolution, as reported by Fig. 14b, it is possible to determine two values of the derivate graphically, which in this case are equal to 0.17 and 0.19, respectively. Knowing that the molar volume of $LiMn_2O_4$ is equal to 42.3 cm^3/mol and using expressions 17 and 18, it is finally possible to determine the diffusivity at this potential values summarized in Table 2.

PITT and Spherical Coordinate Fick Equation Resolution (SCFER)

Using a Mac-Pile-II Biologic potentiostat–galvanostat and the relevant software, it is possible to calculate the diffusivity value in a simple manner, which is by means of the expression 8.

Table 7 Coefficient diffusion repeatability

Method	$LiFePO_4$ 3.47 V D (cm^2/s)	$LiMn_2O_4$ 4.01 V D (cm^2/s)	$LiMn_2O_4$ 4.13 V D (cm^2/s)
PITT and Cottrell region	3.2×10^{-14}	2.6×10^{-9}	
PITT and Cottrell region	1.8×10^{-14}	5.5×10^{-9}	5.2×10^{-9}
PITT and Cottrell region	2.2×10^{-14}	8.1×10^{-9}	9.0×10^{-9}
PITT and Cottrell region	5.9×10^{-14}	3.8×10^{-9}	6.5×10^{-9}
PITT and Cottrell region	4.2×10^{-14}	2.8×10^{-9}	
PITT and Cottrell region	3.6×10^{-14}	5.3×10^{-9}	
Impedance spectroscopy	2.0×10^{-14}	3.7×10^{-9}	
Impedance spectroscopy	6.8×10^{-14}	2.3×10^{-9}	2.3×10^{-9}
Impedance spectroscopy	5.3×10^{-14}	1.5×10^{-9}	8.2×10^{-9}
Impedance spectroscopy	4.0×10^{-14}	1.6×10^{-9}	5.4×10^{-9}
Impedance spectroscopy	3.3×10^{-14}	3.0×10^{-9}	
Impedance spectroscopy	1.0×10^{-14}	2.4×10^{-9}	
PITT and SCFER	1.2×10^{-14}	3.1×10^{-9}	
PITT and SCFER	6.3×10^{-14}	6.0×10^{-9}	3.1×10^{-9}
PITT and SCFER	4.1×10^{-14}	3.7×10^{-9}	4.5×10^{-9}
PITT and SCFER	5.7×10^{-14}	6.2×10^{-9}	7.1×10^{-9}
PITT and SCFER	7.7×10^{-14}	4.2×10^{-9}	
PITT and SCFER	8.3×10^{-14}	4.3×10^{-9}	

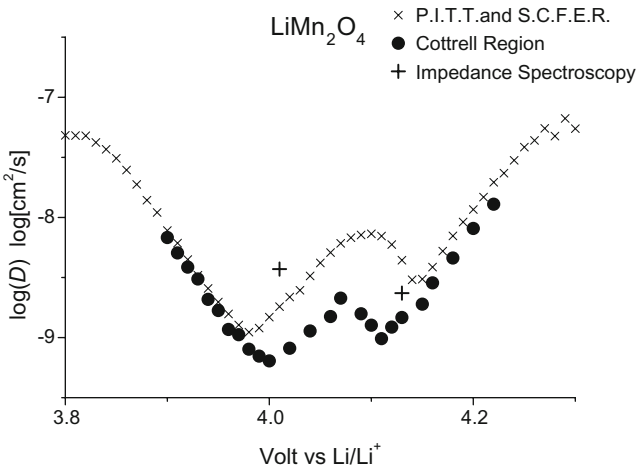

Fig. 15 Diffusion coefficient values of $LiMn_2O_4$ vs. potential

By processing the file raw in a specific way, indeed, it is possible to obtain data concerning any cyclic voltammetry step. Each step maintains a constant potential value, and it is therefore possible to obtain information about the current variation with the time, charge intercalated or deintercalated, and so on. But, our interest is focused on the two abovementioned first parameters. As has been defined before, α is the ratio between the real and theoretical values of the capacity.

Without performing any data processing, this parameter can be directly used inside relation 8. In Table 5, the parameter values recorded during the step at 3.47 V for $LiFePO_4$ and at 4.01 and 4.13 V for $LiMn_2O_4$ have been reported. Therefore, the diffusion coefficient calculated in this case for $LiFePO_4$ at 3.47 V [22] and the diffusion coefficients calculated instead for $LiFePO_4$ at 4.01 and 4.13 V are, respectively, shown in

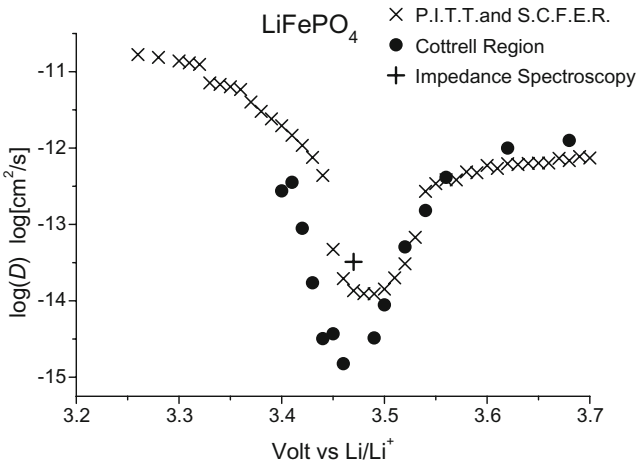

Fig. 16 Diffusion coefficient values of $LiFePO_4$ vs. potential

Table 6. Finally, Table 7 summarizes the results of a certain number of experiments (done at same voltage value) to calculate the diffusion coefficient and highlights that they are quite close to the values reported in literature [15, 21, 23, 24] and each other.

Moreover, the diffusion coefficient as a function of the potential has been reported in Figs. 15 and 16, highlighting a similar shape of the curves obtained by the expression 8 and by PITT–Cottrellian technique for both materials. The same shape has also been found in literature [3, 5, 25] for $LiMn_2O_4$ and $LiFePO_4$. Indeed, only a single value of the diffusion coefficient measured by the EIS technique in correspondence of the cyclic voltammeter peaks has been reported, for both materials confirming, in any case, the goodness of our conclusions.

Conclusion

By using a scanning electron microscope the particle size and shape, which has been ideally assumed as spherical for both materials considered in this work, have been evaluated to approach the diffusion problem. Measuring and determining, more times, the diffusion coefficient by different techniques (PITT and impedance spectroscopy) and by solving Fick's equation through the spherical coordinates, our approach to determine the diffusion coefficient, by using expression 8, has been proven correct. Levi and Aurbach demonstrated the equivalence in application of the three differential techniques PITT, galvanostatic intermittent titration technique, and EIS [26], and we started from this point to reach to our conclusions. It is also worth noting instead that the knowledge of the diffusion coefficient allows having an idea of particles' dimension.

Appendix

The solution has this form: $c(r,t)=X(t)Y(r)+K_1$.

$X(t)$ is only t dependent, $Y(r)$ is only r dependent, and K_1 is a constant:

$$\frac{\partial X}{\partial t}Y = D\frac{1}{r^2}\frac{\partial}{\partial r}\left(r^2\frac{\partial Y}{\partial r}\right)X \tag{19}$$

$$\frac{\partial X}{\partial t}\frac{1}{X} = D\frac{1}{r^2}\frac{\partial}{\partial r}\left(r^2\frac{\partial Y}{\partial r}\right)\frac{1}{Y} \tag{20}$$

the left side of the Eq. 20 is only a function of the time, while the right side is only a function of the radius. Therefore, both parts have to be constant, and the solution is:

$$c - K_1 = C_1\exp(-Kt) \times \frac{A\exp\left(i\sqrt{\frac{K}{D}}r\right) + B\exp\left(i\sqrt{\frac{K}{D}}r\right)}{r} \tag{21}$$

Because this equation must be also valid when $r=0$, we impose $A=-B$, and then assuming $C_1A=C_2$, we have:

$$c - K_1 = C_2\exp(-Kt)\frac{\exp\left(i\sqrt{\frac{K}{D}}r\right) + \exp\left(i\sqrt{\frac{K}{D}}r\right)}{r} \tag{22}$$

assuming $C_2 = \frac{K_2}{2i}$ to have a real solution and knowing that

$$\exp(x+iy) = \exp(x)[\cos(y) + i\sin(y)] \tag{23}$$

we can write:

$$c - K_1 = K_2\exp(-Kt)\frac{\sin\left(\sqrt{\frac{K}{D}}r\right)}{r} \tag{24}$$

$\sqrt{\frac{K}{D}}R = \lambda\pi$ for $\lambda=1$, $K = \frac{\pi^2 D}{R^2}$ and therefore:

$$c - K_1 = K_2\exp\left(-\frac{\pi^2}{R^2}Dt\right)\frac{\sin\left(\frac{\pi}{R}r\right)}{r} \tag{25}$$

the boundary conditions are:

$$t \to 0;\ r = R;\ c = c_s \Rightarrow \quad K_1 = c_s \tag{26}$$

$$t \to 0;\ r = 0;\ c = c_0 \Rightarrow K_2 = \frac{(c_0 - c_s)R}{\pi} \tag{27}$$

so:

$$c_s - c = \frac{(c_s - c_0)R}{\pi}\exp\left(-\frac{\pi^2}{R^2}Dt\right)\frac{\sin\left(\frac{\pi}{R}r\right)}{r} \tag{28}$$

References

1. Wen CJ, Boukamp BA, Huggins RA, Weppner W (1979) J Electrochem Soc 126:2258
2. Deiss E, Häringer D, Novak P, Haas O (2001) Electrochim Acta 46:4185
3. Tang XC, Song XW, Shen PZ, Jia DZ (2005) Electrochim Acta 50:5581
4. Tang XC, Pan CY, He LP, Li LQ, Chen ZZ (2004) Electrochim Acta 49:3113

5. Deiss E (2002) Electrochim Acta 47:4027
6. McKinnon WR, Haering RR (1987) Modern aspect in electrochemistry. Plenum, New York
7. Ho C, Raistrick ID, Huggins RA (1980) J Electrochem Soc 127:343
8. Bauer EM, Bellitto C, Righini G, Pasquali M, Dell'Era A, Prosini PP (2005) J Power Sources 146:544
9. Bellitto C, Bauer EM, Righini G, Green MA, Brandford WR, Antonini A, Pasquali M (2004) J Phys Chem Solids 65:29
10. Antonini A, Bellitto C, Pistoia G (2001) US Patent no. 6274279
11. Xia Y, Zhou Y, Yoshio M (1997) J Electrochem Soc 144:2593
12. Robertson AD, Lu SH, Howard WF (1997) J Electrochem Soc 144:3505
13. Weppner W, Huggins RA (1977) J Electrochem Soc 1569:1578
14. Levi MD, Levi EA, Aurbach D (1997) J Electroanal Chem 421:89
15. Srinivasan V, Newman J (2004) J Electrochem Soc 151:A1517
16. Montella C (2002) J Electroanal Chem 518:61
17. Montella C (2005) Electrochim Acta 50:3746
18. Vorotyntsev MA, Levi MD, Aurbach D (2004) J Electroanal Chem 572:299
19. Brown ER, Sandifer JR (1986) In: Rossiter BW, Hamilton JF (eds) Physical methods of chemistry, 2nd edn. Wiley, New York
20. Pyun SI, Choi YM, Jeng ID (1997) J Power Sources 68:593
21. Saïdi MY, Barker J, Koksbang R (1996) J Solid State Chem 122:195
22. Prosini PP, Zane D, Pasquali M (2001) Electrochim Acta 46:3517
23. Peña JS, Soudan P, Arean CO, Palomino GT, Franger S (2006) J Solid State Electrochem 10:1
24. Pyun SI, Choi YM, Jeng ID (1997) J Power Source 68:593
25. Prosini PP, Lisi M, Zane D, Pasquali M (2002) Solid State Ionics 148:45
26. Levi MD, Aurbach D (1999) Electrochim Acta 45:167